4-1-2021

Influence of Bulk and Surface Interactions from Thick, Porous, Soil-based Substrates on the Spreading Behavior of Different Viscosity Oils

Firoz Ahmed
University of Mississippi

Brenda Hutton-Prager
University of Mississippi

Recommended Citation

Ahmed, F., & Hutton-Prager, B. (2021). Influence of bulk and surface interactions from thick, porous, soil-based substrates on the spreading behavior of different viscosity oils. Environmental Challenges, 3, 100045. https://doi.org/10.1016/j.envc.2021.100045

Environmental Challenges 3 (2021) 100045

Contents lists available at ScienceDirect

Environmental Challenges

journal homepage: www.elsevier.com/locate/envc

Influence of Bulk and Surface Interactions from Thick, Porous, Soil-based Substrates on the Spreading Behavior of Different Viscosity Oils

Firoz Ahmed, Brenda Hutton-Prager*

University of Mississippi, Chemical Engineering Department, 140 Anderson Hall, University, MS 38677, USA

ARTICLE INFO

Keywords:
Crude oil
Motor oil
Spreading kinetics
Wettability
Contact angle
Thick porous substrates

ABSTRACT

Crude oils and motor oils are commonly identified in oil spills on land. Controlling and understanding their flow both across and into land is of paramount importance to minimize spread and subsequent damage to the ecosystem. Spreading kinetics and surface energy studies were conducted with these oils over several realistic soil-based matrixes, consisting of topsoil (silt-dominant), sand, clay, and moisture. Spreading area through a 1.3 cm deep matrix was reduced with increased moisture content, densely packed matrixes, and higher viscosity oils. Initial contact angle (CA) measurements for all oils was typically lower on clay matrixes due to its sheet-like structure and high absorption capabilities. Individual droplet penetration took longer at lower MC in direct contradiction to bulk kinetics studies, suggesting different spreading behavior across the surface border. Low viscosity oils recorded the highest lateral spreads, and incomplete wetting profiles were identified for most conditions tested. Importantly, dimensionless profiles of droplet diameter and CA with time did not conform to universal behavior, with statistically significant influences of matrix heterogeneity, oil viscosity, and ill-controlled surface roughness identified. Flow regimes of oil droplets instead conformed to vertical spreading through thick matrixes, and a delayed lateral spreading that occurred quite late into the total penetration time of the droplet. These findings, obtained from studying realistic soil-based matrixes, draws new conclusions regarding the important influences of matrix thickness, variable porosity, and chemical heterogeneity on fluid flow behavior. This new knowledge will assist in the development of future containment efforts surrounding oil spills.

1. Introduction

Soil is a vital element of the ecosystem, and is a mixture of different minerals, organic matter, liquids, gases, and microorganisms. Its delicate habitat can be irreversibly damaged from oil-based contamination by industrial or commercial spills, waste treatment, oil extraction/production, or inferior goods storage (Guimarães et al., 2010).

There have been many notable oil spills over several decades. The 1989 Exxon Valdez Tanker leakage released 37,000 tons off the Alaskan coast, however clean-up efforts and investigations of this incident resulted in the 1990 Oil Pollution act (Chen et al., 2019). The Mingbulak oil spill in Uzbekistan in 1992 (USDOE Energy Information Administration, 1995) occurred in the city of Fergana, and 88 million gallons of oil was released. The Niger Delta oil spills occurred over a 50 year period, with a recorded 1.5 million tons lost, confirmed by the Federal Ministry of Abuja and the Nigeria Conservation Foundation in 2006 (Jernelöv, 2010). There were more than 7,000 oil spills in this region between 1970 and 2000, as reported by the Nigerian Federal Government (Jernelöv, 2010). In 1994, the Arctic's largest oil spill on land with 100,000 barrels of oil was recorded in Russia's Komi Republic, 1,000 miles northeast of Mosco (Stone, 1995). In the Komi spill, the amount of oil spilled was three times that released in Alaska's Exxon Valdez catastrophe in 1989 (Stone, 1995). Another notable spill was the northwestern Amazon oil spill, which polluted many areas including rainforests, streams, and rivers of Ecuador, Peru, and Columbia (Jernelöv, 2010). Many of these larger oil spill examples have resulted from crude oil extraction, transportation or refinement operations (Chinenyeze and Ekene, 2015), while smaller spills found on farms are more likely to contain motor oil, with spent oil affecting large farming areas over significant periods of time (Ramadass et al., 2015).

Long-term damage resulting from these and other examples has required long-term remediation efforts to remove the oil from the contaminated soil, including contaminants that have made their way into aquifer systems (Knox et al., 1997). Remediation efforts include bioremediation technology (Guimarães et al., 2010), phytoremediation (Razmjoo and Adavi, 2012) and chemical remediation (Lim et al., 2016). However, more immediate responses following an oil spill are also required to help prevent long-term damage to the fragile soil ecosystem. A study on the toxicity of an oil spill after only seven days revealed a 90% death rate of earth worms at 2% oil contamination, and 100% bacterial inhibition at

* Corresponding author.
E-mail addresses: mahmed2@go.olemiss.edu (F. Ahmed), bhprager@olemiss.edu (B. Hutton-Prager).

https://doi.org/10.1016/j.envc.2021.100045
Received 13 November 2020; Received in revised form 4 February 2021; Accepted 5 February 2021

1% petroleum content (Lim et al., 2016). When crude oil is spilled into a soil environment, it inhibits the diffusion of air particles into the soil pores, creating anaerobic conditions to the detriment of many microorganisms inside the soil (Klamerus-Iwan et al., 2015). Other chemical properties such as pH, temperature, and total organic carbon are also drastically changed due to the presence of oil contaminants (Wang et al., 2013). One important aspect in developing a successful immediate response effort is to better understand how the oils flow across and into the land. Understanding their surface-interactions with realistic land substrates, multi-components and variable porosities is imperative in identifying variables that influence the spread of fluids. Once identified, this information can then be used to develop responses that better minimize the spread.

There are well known theories that describe liquid flow over porous media, such as in the case of oil spills on land. Surface energy considerations are considered with wetting theory, where wetting is possible when the surface energy of the substrate, σ, is equal to or larger than the surface tension of the liquid, γ (Song et al., 2019). The Cassie-Baxter equation relates the observed CA with influencing factors of roughness and heterogeneity of a surface, and is shown in Eq. (1) (Rutter and Hutton-Prager, 2018):

$$cos\theta_b = rcos\theta_0 - f_{LA}\left(rcos\theta_0 + 1\right) \quad (1)$$

θ_b is observed CA, r is roughness, θ_0 is the equivalent CA on a flat surface, and f_{LA} is the fractional area of liquid in contact with a secondary component, which could either be another substrate component or air. This expression works equivalently for a binary component substrate or a pure porous substrate (Milne and Amirfazli, 2012). In the case of the oil and soil interface, the high roughness of the soil matrix and/or its chemical heterogeneity and porosity can help limit the spreading of the oil, depending on the CA range for the system.

The Lucas-Washburn equation relates the effects of liquid properties (viscosity, μ; surface tension, γ) on its flow through a porous solid with a particular capillary height (h) and radius (r), and is given by Eq. (2) (Cummins et al., 2017). This may be used to describe oil spreading phenomena through the pores of a soil substrate. The bulk porosity of the soils is influenced by particle size and particle size distribution (Nimmo, 2013), and is also an important factor in complex soil mixtures that comprise several different components such as sand, silt and clay. These components are of decreasing size respectively (Kettler et al., 2001; Ritchey et al., 2015).

$$h^2 = \frac{r\gamma cos\theta_b}{2\mu}t \quad (2)$$

Several numerical simulations and experimental studies have also been published regarding fluid flow over non-porous and porous media (Alleborn and Raszillier, 2004; Das et al., 2018; Frank and Perré, 2012; Johnson et al., 2019; Starov et al., 2003). While there have been considerable developments in understanding liquid flow over *thin* porous substrates, further work is still required to understand the effects of *thick* porous substrates (Johnson et al., 2019) and also the effects of multicomponents within a substrate (Starov et al., 2003). Starov et al. (2003) presented an in-depth study of both theoretical and experimental investigations of liquid droplets spreading over porous layers. Brinkman's equations, which included effective liquid viscosity and permeability coefficients as semi-empirical parameters, were used to describe liquid flow both across and through the porous layer. These theoretical descriptions were developed for thin porous substrates and a droplet height much larger than the substrate height. Starov et al. (2003) projected similar applicable analyses for small oil droplets spreading across thick porous substrates, and demonstrated a universal curve of droplet radius and CA vs time, all in dimensionless units, for many different systems. This universality condition held true provided that the porous substrates were dry; had similar porosities; and similar pore sizes. It was independent of substrate material; depth of substrate (i.e. thin or thick); and viscosity of fluid. Alleborn and Raszillier (2004) however, provided a different numerical model for liquid droplets spreading over thick, porous substrates, where the depth of substrate was influential to the model considerations. It is also very well known that fluid viscosity is a key property that describes fluid flow. There appears to be differing viewpoints within the literature regarding the variables that influence fluid spreading behavior over porous substrates.

The aim of this study is to identify specific variables of bulk soil substrates and their surfaces that influence the spreading behavior of oils flowing over and into these substrates. Several variables investigated include the moisture content (MC); chemical makeup of the soil substrate (topsoil, sand, clay); and packing density of the substrate (loose and dense packed). The prepared soil samples are typical of land substrates common in some areas of the USA (Schraer et al., 2003), but are chosen simply as a realistic 'model soil' in which to conduct this investigation. Oil viscosity is also chosen as a variable, and three different viscosity oils indicative of those identified during land oil spills were selected: two crude oils (CO-1 and CO-2); and one motor oil (MO). Spreading kinetics studies of oils flowing *through* soil substrates are conducted to assess bulk effects on the fluid transport, while *surface interaction* studies of the substrate with the oil investigate penetration capabilities. These important new findings, which highlight the different and competing influences of bulk and surface interactions on oil spreading behavior, may be used to modify existing flow models of liquid droplets over porous substrates, ultimately progressing the understanding of oil flow behavior over land during oil spills. These developments may also lead to better and more immediate solutions in mitigating environmental damage with the development of suitable materials or solutions that minimize oil spread.

2. Materials and methods

2.1. Materials

MO (Supetech^{TM} SAE 5W -20) was purchased from Walmart superstores, Oxford, MS. CO-1 was generously donated by Ram Petroleum, LLC, located in Tylertown, MS; and CO-2 by Coastal Chemical Co., L.L.C., LA 70518. Quikrette premium play sand and Scotts Premium Topsoil were also purchased from Walmart superstores, Oxford, MS. The topsoil was considered to be dominant in silt, based on a simple procedure done to test the texture of the soil (Ritchey et al., 2015). Natural clay was supplied by the University of Mississippi field station, Abbeville, MS. Petri dishes (90 mm) were provided by Fisher brand. Leur lock BD syringes (3 mL) were used with the CA studies.

2.2. Methods

Basic properties of the oils: The viscosity of CO-1, CO-2, and MO was measured using a controlled stress/strain, Discover HR-2 hybrid rheometer at the Chemical Engineering Laboratory, Mississippi State University (MSU). It was equipped with parallel-plate geometry (set gap: 570 μm, torque: 3.09094×10^{-3} mNm, solvent trap: 500 μm). The temperature of the laboratory was fixed by using a Peltier plate steel – 105471 system at 22°C. Each sample was placed in the plate by a 1 mL plastic dropper at the edge of the plate and cleaned with a cotton bud if the oil spilled. All rheological tests were performed at least twice for repeatability purposes. Oil density was measured according to ASTM D 1475-98(2003) at a constant temperature of 24°C. The method was first calibrated and confirmed with water as per the test procedure. Measurements were performed in triplicate. Surface tension of the oils was measured using the pendant drop method on a Biolin Scientific OneAttension CA analyzer, with NAVITAR camera and OneAttension software. Again, all measurements were done in triplicate.

Preparing the matrixes: For the purposes of discussion and identification, from hereon in, a mixture matrix will comprise of topsoil, sand, and clay (and water where applicable); while individual substrates will be referred to as a topsoil matrix, a sand matrix, and a clay matrix. These

Table 1
Composition of loosely and densely packed mixture matrixes. Water was added to the dry mixture for MC studies. The combined composition of the three soil components resulted in a clay-based soil overall, based on the USDA soil texture triangle (Ritchey et al., 2015) and mimicking clay-based soils in MS (Schraer et al., 2003).

Components	Loosely packed composition (63 g total as dry basis)	Densely packed composition (70 g total as dry basis)
Clay	50% (31.50g)	50% (35.00g)
Sand	35% (22.05g)	35% (24.50g)
Topsoil	15% (9.45g)	15% (10.50g)
Water – 5% MC	3.32 g	3.68 g
Water – 10% MC	7.00 g	7.78 g

latter substrates are prepared to better understand the chemical influences of each component in the mixture matrix on oil spreading at the oil-soil interface.

Topsoil, sand and clay were initially placed in a Precision oven for 48 h to remove existing moisture. To prepare mixture matrixes for *spreading kinetics experiments*, topsoil and sand were sieved using a 5 mm sieve (Fisher Scientific) to remove oversized particles. Each component was then weighed according to the amounts given in Table 1 for loose or dense packed matrixes, using an Adventurer™ brand electronic scale. Components were then mixed for 5 minutes with a stainless-steel spatula, and transferred to an 87 mm petri dish base (Fisher brand). To prepare matrixes with 5 or 10% MC, the amount of water was calculated on a wet basis and added during the mixing step. The formulae used for this calculation are given by Eqs. (3) and (4):

$$\mathrm{MC} = \frac{M_w - M_d}{M_w} \times 100 \tag{3}$$

$$H_2O = M_w - M_d \tag{4}$$

where MC is the moisture content (%) of the material; M_w is the wet mass of the mixture, M_d is the mass of the mixture after drying, and H_2O is the mass of water added to prepare the targeted mixture.

Matrixes prepared for surface interaction experiments included individual component matrixes as well as mixture matrixes with the same composition as shown in Table 1. Clay and topsoil were ground – rather than sieved – using a mortar and pestle to create uniform particle size. Matrixes were prepared dry and with 5 and 10% MC to assess the effect of moisture on CA. The dry basis mass for all preparations (individual and mixture matrixes) was 63.69 g to completely fill a 90 mm petri dish lid (Fisher) and generate a flat surface at constant packing.

Porosity and Density of the Matrixes: Porosities were estimated using a simple method cited by Matko (2003), where known amounts of water were poured over dry prepared matrixes in the petri dishes (or lids) until it reached the top. The volume of water, divided by the volume of the petri dish (or lid), provided an indication of each substrate's porosity. While it is acknowledged that some of this water may have become bound to one or more of the components within the matrix, this estimation was performed for relative comparison across the matrixes prepared. The method followed appears widely used in such estimations. Densities of each matrix were determined by dividing the mass of contents added to the petri dish (or lid) by its volume.

Spreading kinetics experiments: For densely packed trials, the mixture matrix was pressed by hand into the petri dish until it was the same height as the petri dish walls (1.3 cm). With the loosely packed trials, no pressure was needed to spread the contents into the dish. The mixture matrixes were horizontally mounted above digital imaging facilities (f/2.0, 28 mm, autofocus with LED flash) to video-record the oil spreading process through the matrix at a depth of effectively 1.3 cm, from the base of the petri dish. Recording was maintained for 20 min. The oil (10 mL) was poured onto the mixture matrix surface from above, at a vertical distance of 7.0 cm and a rate of approximately 20 mL/min. Oil quantity was large enough to create a puddle, but small enough not to spread to the edges of the petri-dish container. Still images were extracted from the resulting video every 30s and exported into ImagePro Premier (v9.2 software), where the oil spreading area was quantified. All spreading experiments were done in triplicate, and one standard deviation in the area determinations was not more than ± 0.9 cm^2.

Surface interaction experiments: A Biolin Scientific OneAttension Contact Angle (CA) analyzer, with NAVITAR camera and OneAttension software, was used to perform dynamic CA and baseline measurements of sessile oil droplets placed on topsoil, sand, clay, and mixture matrixes, with and without MC. Oil droplets were delivered manually using the disposable syringes to prevent contamination between each oil, and the average droplet size delivered for each oil was 27.7 ± 1.3 μL. All surface measurements were done in triplicate, and one standard deviation was routinely no more than ± 5° for the CA, and ± 1.6 cm for the baseline, defined as the droplet diameter in contact with the matrix surface at any given time.

Statistics Analysis: 3-way ANOVA was applied to both sets of results (spreading kinetics and surface energy data) using Minitab ®, 19.2020.1, © 2020. Individual influences (matrix, MC, oil type) and dual influences of these parameters were investigated. The null hypothesis was that the means of all populations compared were equal, while the alternate hypothesis was that one or more of the population means compared were not equal. A significance level of $\alpha = 0.05$ was used for all analyses, and the inverse cumulative distribution function (ICDF) of the Chi-Square distribution was used to calculate critical F values (F_{crit}). Hypotheses were accepted or rejected by comparing the calculated F values (F_{calc}) in the statistics analyses with F_{crit}. The R^2 of all statistics models created for each condition ranged between 91.00 and 98.43% except for one condition, which was 87.86%. Hence all models were considered excellent fits of the experimental data.

3. Results and discussion

3.1. Properties of oils and matrixes

The average steady-state viscosity of the oils chosen for this investigation was observed after 10 s^{-1} at a temperature of 22°C, and the constant viscosity values are reported in Table 2. All oils displayed linear viscoelastic behavior within the shear rate range under which they were tested. Densities and surface tensions, measured at 24 °C, are also reported in Table 2.

The composition of the crude oils are mostly hydrocarbons with carbon number ranging from $C_5 - C_{15,}$ and include resins, asphaltenes, saturates, aromatics, and napthene compounds, the latter of which is almost 10% of the total composition (Chinenyeze and Ekene, 2015). Motor oils typically contain hazardous additives including zinc, magnesium (Ramadass et al., 2015), dithiophosphates, calcium sulphonates, succinimide dispersants, and polymeric viscosity modifiers (Herdan, 1997), which may interact with the matrix components and influence fluid flow behavior. Several of these additives increase the emission of hydrogen sulfide (H_2S), chlorine sulfur, and hydrogen chloride (HCl) in the environment (Herdan, 1997).

The densities and porosities of each matrix prepared are shown in Table 3. Porosities were measured only for the dry matrixes (i.e. 0% MC), and may be influenced by water becoming bound to some of the soil components (Savage and Liu, 2015). However, they serve as a useful relative comparison amongst the different matrixes prepared. The porosity of several marine sands off the coast of Florida, measured using imaging techniques, was reported as low as 37.7% (Curry et al., 2004), a little higher but reasonably close to the value reported in Table 3. Another reference (Ghanbarian et al., 2016) has sand porosity at 35.4%. Likewise, the mass ratio for total porosity of clays (defined as mass of water / mass of water plus clay) was reported as approximately 0.3 by Savage and Liu (2015), for a density of 1250 kg/m^3 (the same density used in the present study). When converting the reported volume-based porosity for clay in Table 3 into a mass-based porosity, this value comes

Table 2
Viscosity, density, and surface tension of the three oils, together with their respective errors of 1 standard deviation.

Type of Oil	Measured viscosity (Pa.s)	Measured density (kg/m^3)	Surface Tension (mN/m)
CO-1	0.5299 ± 0.0058	926 ± 2	40.44 ± 2.20
MO	0.0949 ± 0.0225	850 ± 1	37.75 ± 0.25
CO-2	0.0089 ± 0.0004	840 ± 1	33.18 ± 0.24

Table 3
Densities and porosities of dry matrixes. One standard deviation is shown for the porosity measurements. Densities were calculated from the matrix masses divided by the calculated volume. A typical error in mass measurement can be assumed ± 0.02 g.

Matrix	Density (g/cm^3)	Porosity (vol%)
Loosely packed	0.76	66 ± 2
Densely Packed	0.84	59 ± 1
Top Soil	1.25	41 ± 2
Sand	1.25	33 ± 1
Clay	1.25	68 ± 3
Mixture	1.25	67 ± 2

to 0.35, which is again quite close. The propensity of clay to adsorb water results in a higher-than-expected porosity (vol%), regardless of particle size (coarse or ground). Silt loam was quoted as low as 44.2% (Ghanbarian et al., 2016), which is similar in composition to the top soil used. Although impossible to discern whether or not the samples referenced by literature were identical to those used in the present study, both sets of values notionally confirm that the porosity measurements reported in Table 3 correlate well with other data.

Polydisperse mixtures of different components have higher porosity and often a larger pore size distribution than monodisperse mixtures, and those with irregular-shaped particles also tend to increase the porosity (Nimmo, 2013). The loosely and densely packed matrixes had larger particles sizes (up to 5 mm) compared with matrixes where the components were ground down, and hence resulted in larger porosity values. However, this trend was not observed with the clay or mixture matrixes. Clay is known to readily adsorb water due to its plentiful –OH groups (Savage and Liu, 2015), and likely explains the breakdown in trend for this matrix. Clay particles, however, are also the smallest of the three components (Kettler et al., 2001; Ritchey et al., 2015), and are prone to aggregate, forming larger pore sizes between aggregates (Nimmo, 2013). It is possible that the ground mixture matrix may have formed powdered aggregates, causing much larger pores than might otherwise have been expected with a more uniform particle-size matrix. The resulting mixture matrix for surface studies therefore had a similar porosity to the loosely packed matrix used for kinetics studies.

3.2. Variables affecting oil spreading kinetics through bulk mixture matrixes

Mixture matrixes were prepared with topsoil, sand and clay, as well as differing MC to fully explore the spreading kinetics of oil puddles through these matrixes. For each variable investigated, spreading profiles plotting the cumulative area of spread with time were recorded as raw data, and an example is shown in Fig. 1 for densely packed matrixes. As seen from these traces, there is a time delay before oil spreading is first noticed, corresponding with the oil penetration kinetics through the 1.3 cm deep matrix. This delay differs with MC, oil viscosity, and matrix density (or equivalently, porosity). Spreading areas were also observed to vary with these same parameters, and the cumulative spreading plots with time essentially showed a normal distribution for many of the plots (Bowling et al., 2009). The medium viscosity oil, MO (Fig. 1b)) tended to show less influence with MC on spreading rates compared with the two crude oils. This may be attributed to the additives frequently introduced in such lubricant oils, comprising up to 10% of the total composition (Ramadass et al., 2015) and often including detergents or dispersants (Hamad et al., 2004; Ramadass et al., 2015), depending on MO brand. The detergents especially may have assisted MO miscibility with the moisture, subsequently overcoming, at least partially, the oil-water immiscibility phenomenon.

Statistical analyses investigating the individual and combined effects of matrix packing, MC, and oil type, showed that the time of first recorded spread was strongly influenced by all three variables when considered individually (irrespective of the other two variables). The strongest influence of these was the oil type, followed by MC and finally matrix packing. This indicates that oil properties such as viscosity and surface tension played a dominant role in influencing its movement through the matrix. Packing, and hence porosity, of the matrixes, had the least influence in this response variable, although was still deemed statistically significant. The spreading area at 1000 s was arbitrarily chosen as a constant data point to quantitatively compare spreading kinetics over different conditions. Statistical analysis of this data showed that only the influence of MC was dominant in affecting the spreading area. The main effects data for both these responses is shown in Fig. 2.

While many of these observations are intuitive, they also serve to validate the experimental methods chosen for this work. The data provided a snapshot of various influences on spreading kinetics and spreading area *through* the matrixes, at a cross-section positioned 1.3 cm from the surface. The viscosity of an oil reflects its ability to flow, and hence low viscosity oils more quickly flowed through a given matrix than a higher viscosity oil. Additionally, oils with higher surface tensions were less likely to wet a surface if these values surpassed the surface energy of the matrix. The surface tensions of the three oils were reasonably similar in value, and therefore it is likely that viscosity was the dominating factor affecting kinetics of flow. The Lucas-Washburn expression (Eq. (2)) confirmed these initial observations, demonstrating increased penetration times with increased viscosities, all else being approximately equal. As MC increases within the matrix, an oil-water immiscibility develops, and has the effect of slowing down the spreading kinetics as well as minimizing the area of the spread. Finally, loosely packed matrixes were more porous and less dense (see Table 3), and therefore allowed fluids to flow more quickly through their depth, hence explaining quicker times for the first observance of spread. Table 4 summarizes the influences of the main variables under consideration on the responses measured, for all studies discussed in this paper.

3.3. Surface and interfacial variables affecting oil droplet spreading and penetration

In this section, we characterize the influences of the matrix surface and interface between the oil and matrix on its spreading and penetration capabilities. Matrixes were prepared both as mixtures and as individual components to understand the chemical influences of matrix components at the interface. MC and oil type were also investigated in a similar manner to the previous spreading kinetics work. For practical purposes, the matrix components needed to be ground into smaller size to enable CA measurements, however porosity values for the mixture matrixes were still very similar to the loosely packed matrixes in the kinetics trials (see Table 3). Five parameters were investigated for their response to the mixture matrix components, MC, and oil type of the droplet: 1) initial CA; 2) time at which the CA reached 20^o; 3) initial baseline (droplet diameter) of the droplet upon contact with the matrix

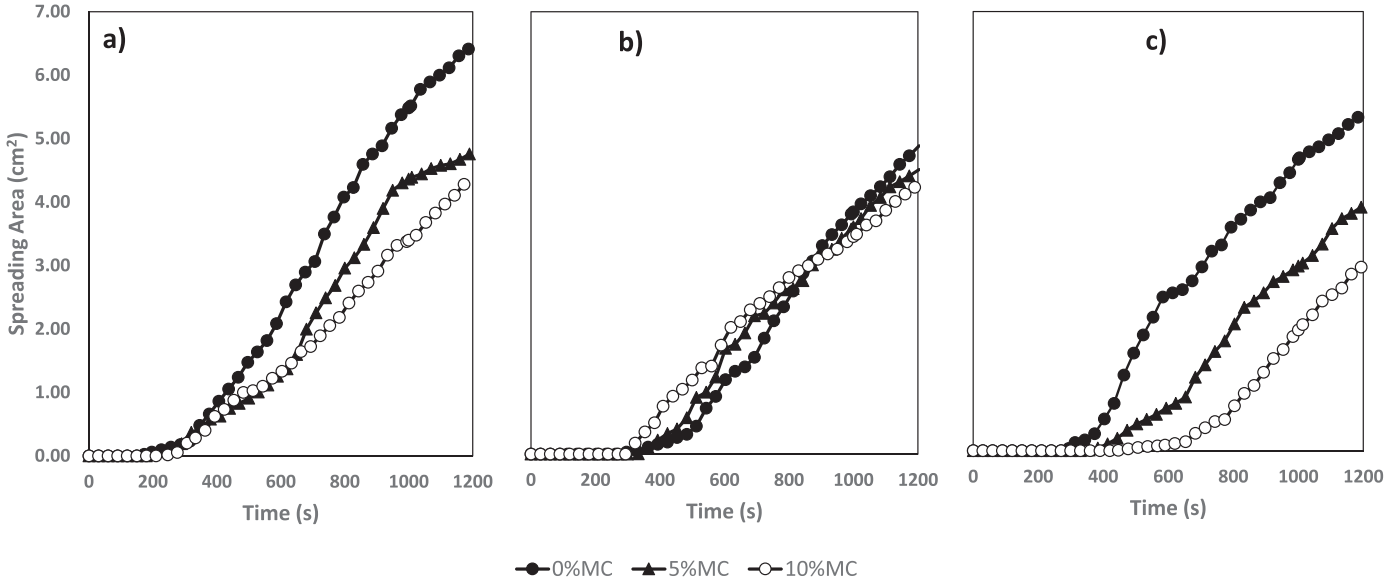

Fig. 1. Example of spreading kinetics profiles of a) low viscosity oil, CO-2; b) medium viscosity oil, MO; and c) high viscosity oil, CO-1, obtained over densely packed mixture matrixes at different MC. The spreading area (y-axis) is the area of oil spread with time measured from the underside of the 1.3 cm thick mixture matrix, with an experimental error no more than ± 0.9 cm^2.

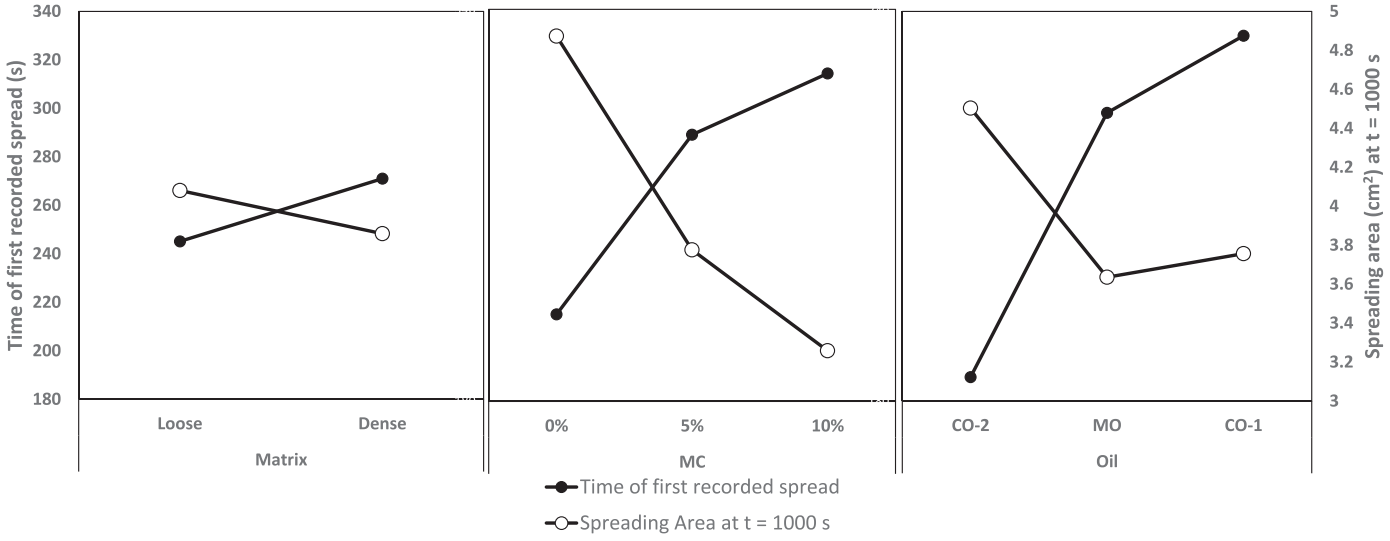

Fig. 2. Statistical analysis of the spreading kinetics data, showing the influences of matrix type, MC, and oil type on the time of first recorded spread (primary y-axis) and spreading area at 1000 s (secondary y-axis). All variables are statistically significant for the time of first recorded spread, while only the MC is significant for the spreading area.

surface; 4) maximum baseline; and 5) time taken to reach maximum baseline. The 20° CA was arbitrarily chosen to quantitatively compare the kinetics of droplet penetration across conditions. All were statistically analyzed using 3-way ANOVA.

The initial CA was strongly influenced by the matrix components and MC, with MC being more dominant than the components themselves, as shown in Fig. 3**a)**. Higher MC resulted in an increase in σ of the matrix, reducing wetting capabilities and hence leading to a higher CA value (Song et al., 2019). Fig. 3a) also highlights a considerably lower initial CA for clay matrixes (irrespective of oil type and MC) and MO oil (irrespective of matrix and MC); and the considerably higher initial CA for mixture matrixes. The sheet-like geometry of clay and its abundance of –OH groups (Uddin, 2008) enables adsorption of several components that can H-bond (Djomgoue and Njopwouo, 2013), and cationic exchange with organic-cations also improves sorption capacity of organic molecules (Katusich et al., 2016). These properties have prompted investigations into the capabilities of clay to help contain land oil spills (Katusich et al., 2016), and may also explain the obvious reduction in initial CA of the oils when in contact with clay substrates. The reduction in initial CA for the medium viscosity oil (MO) could be due to the contribution of several additives within this oil, as outlined earlier. Finally, the much higher initial CA for mixture matrixes is due to the additional effects of chemical heterogeneity and high porosity, as confirmed via Cassie-Baxter theory (Mohamed et al., 2015) (Eq. (1)). For a situation where beading of a liquid is already occurring on a given surface, this beading is further promoted due to the presence of roughness and heterogeneity, created either by multiple chemicals at the surface or increased surface porosity (Rutter and Hutton-Prager, 2018).

The time taken for the CA to reach 20° was strongly influenced by the matrix components, with F comparisons: $F_{calc} >> F_{crit}$ (120.43 >> 7.81); followed by oil type (66.35 >> 5.99); combined influence of matrix components and oil type (29.32 > 12.59); and finally, the MC (11.01

Table 4
Overall summary identifying the relative influence (weak, medium, strong) of considered variables on the responses measured in the spreading kinetics study; the surface interactions study; and existing theoretical models of fluid flow behavior cited in the literature. * Also a combined effect that was statistically significant.

Spreading Kinetics Study		
Variables Investigated	Time of first Recorded Spread	Spreading Area
Moisture Content (MC)	Medium	Strong
Matrix Packing Density	Weak	None
Oil Type (viscosity)	Strong	None

Surface Interactions Study					
Variables Investigated	Initial CA	Time at CA = 20°	Initial Baseline	Maximum Baseline	Time at Maximum Baseline
MC	Strong	Weak	None	None	Weak
Substrate Type (chemistry)	Medium	Strongest*	None	None	Strong
Oil Type (viscosity)	None	Strong*	Strong	Strong	Medium

Theoretical Models of Fluid Flow Behavior	
Variables Considered	Universality of Flow Behavior
MC	Increased MC reduced universality
Substrate Type (chemistry)	Increased heterogeneity reduced universality
Oil Type (viscosity)	More complex components within oil reduced universality

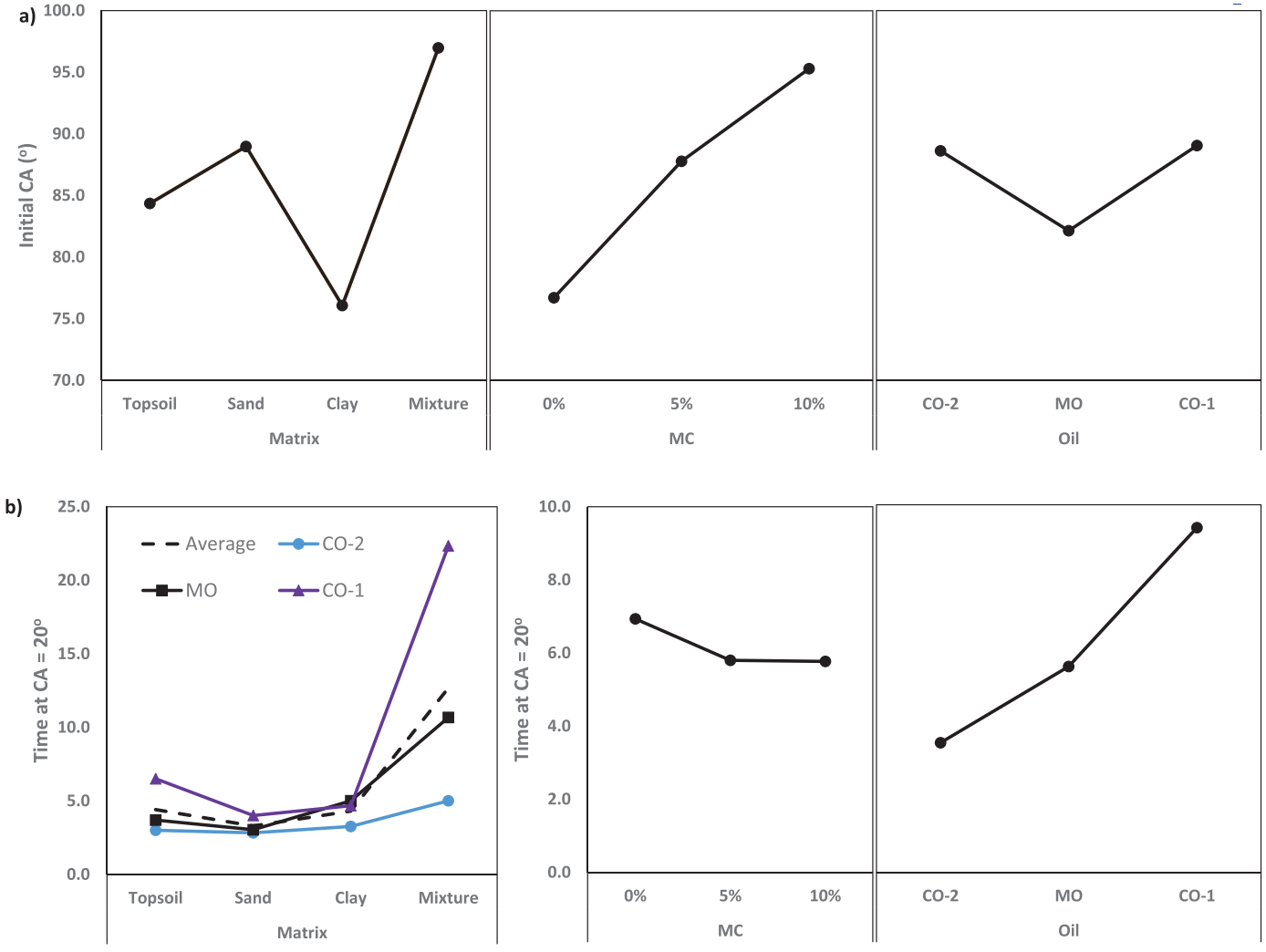

Fig. 3. **a)** Main effects of matrix type, MC, and oil type on the initial CA of oil droplets contacting the matrix surface. Initial CA are averaged across two variables, and plotted against the third. These plots show statistically significant effects of matrix type and MC on the initial CA. **b)** Main effects of matrix type, MC, and oil type on the time taken for the CA of the oil droplets to reach 20°. All three individual variables were shown to be statistically significant in the response time, with MC being the least significant of the three. Combined influences of matrix and oil types were also found to be statistically significant in influencing the response time.

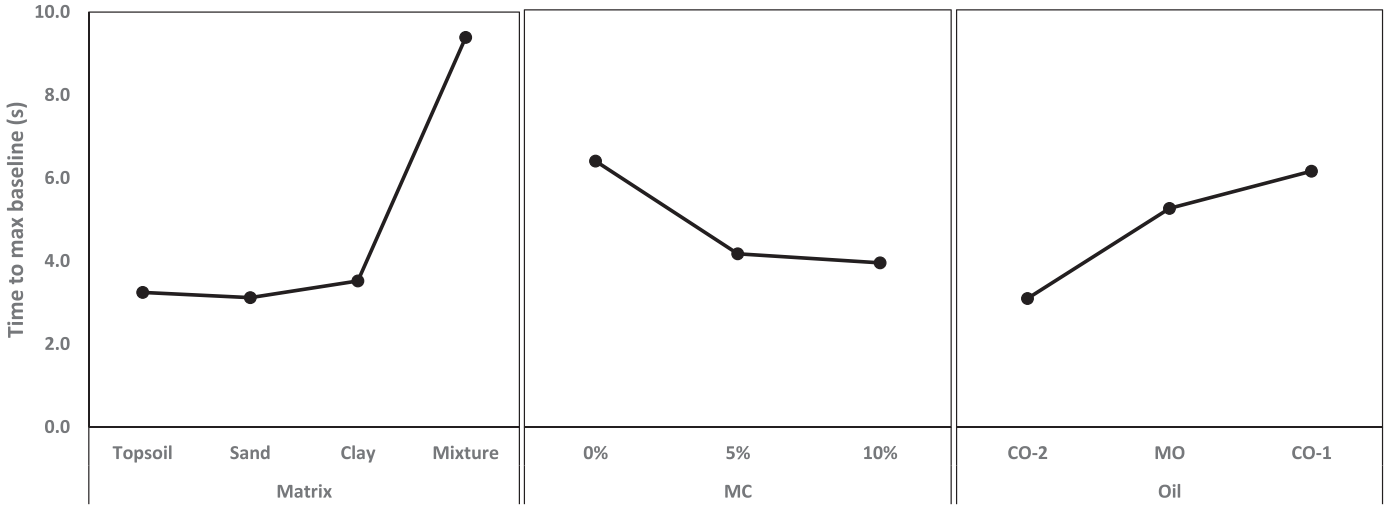

Fig. 4. Main effects of matrix type, MC, and oil type on the time to reach maximum baseline of oil droplets contacting the matrix surface. These times are averaged across two variables, and plotted against the third. Plots show statistically significant effects of matrix type, oil type, and finally MC on the recorded time of the maximum baseline.

> 5.99). These effects are summarized in Fig. 3**b)**, clearly showing that the mixture matrix had the most effect on the resulting penetration time for a given oil, further accentuated by higher viscosity oils with reduced flow capabilities. The analysis showed that while the initial CA is essentially affected by the contact first made with the surface (matrix component, with or without moisture), travel of the droplets through the matrix clearly depended on the matrix as well as the flow characteristics of the oil. While MC affected the initial CA made with the surface, this was less important than the flow properties of the oil when penetrating through the matrix.

Statistical analysis of the baseline data showed that the initial baseline was strongly affected only by the oil type, where trends were more pronounced with clay and mixture matrixes. Higher viscosity (less ability to flow) and higher surface tension (more likely to bead up on a surface) oils consistently generated lower initial baselines, as expected. The lower values frequently observed with the medium viscosity oils (MO) were likely affected by the additives present, as described earlier (Fig. 1b)). The maximum baseline data was the only set of data where the R^2 value was just below 90%, and this value was also strongly affected by the oil type.

The time taken to reach the maximum baseline was individually influenced by matrix type, oil type, and MC, in that order. This mimics the ANOVA results for time taken to reach a CA of 20°, with the exception that the CA was additionally influenced by the combined influence of the matrix and oil types. A more complex or chemically heterogeneous mixture matrix accounts for an increase in tortuosity of penetrating fluids, hence influencing surface observations by longer times to reach a CA of 20° and maximum baseline of the droplet. Additionally, higher viscosity oils also are less able to flow freely through a matrix, and take longer time.

The main effects influencing time to maximum baseline are plotted in Fig. 4, and it is again seen that the mixture data is significantly different from the remaining matrix components, leading to the rejection of the null hypothesis. The differing porosities of each matrix did not appear to influence times required to reach the maximum baseline, with topsoil and sand having relatively low porosities, and clay and mixture matrixes having much higher porosities. The difference between maximum and initial baseline values was determined to be experimentally significant for all conditions tested with low viscosity oils. This was significant only half the time for medium viscosity oils, and not significant for any high viscosity oils, suggesting that the oil viscosity impacts its spreading capabilities in the lateral direction (data not shown).

The least dominant influence of MC – but one that was still recorded as statistically significant – was opposite to expected trends. Both analyses of penetration time responses showed that for any matrix or oil type, higher MC corresponded to quicker times to reach a pre-defined penetration level (low CA or maximum baseline). This is in direct contradiction to the results obtained from the spreading kinetic studies, where it was clear that higher MC resulted in longer times being recorded for first recorded spread, and smaller spreading areas. The kinetics studies essentially represent a snapshot of oil penetration at a certain cross-section depth into the matrix, while the latter study investigates surface influence on the ability of the oil to penetrate into the depths of the matrix. Although the particle sizes were necessarily different between the two studies, their resulting porosities were similar (for multicomponent matrixes), enabling qualitative comparisons of surface and bulk influence on oil spreading behavior. Refer again to Table 4, which summarizes all of these findings for easy reference.

Several studies of other systems have identified significant differences between surface and bulk porosity (Kiefer et al., 2013; Lee et al., 2018), to the extent that surface porosity was influential in controlling material transport of components across the interface into the bulk material. In one study (Kiefer et al., 2013), the surface porosity distribution differed by up to ± 30% of its mean value compared with the bulk porosity, which was largely constant. Adding moisture to a soil sample, presumably at constant density, is known to increase the overall porosity, as the water causes various soil components to compress and hence increase the void space (Abed Gatea Al-Shammary et al., 2020). While this also may seem somewhat counter-intuitive, the larger pore sizes or channels created may be more readily formed at or near the surface given the greater variability in porosity compared with the bulk material. It is therefore plausible that increased MC may provide a more rapid pathway of penetration for individual oil droplets upon surface contact, irrespective of oil and matrix component type (refer to MC graphs in Figs. 3b and 4). Ultimately, the apparent contradictions observed may in fact be a result of the largely different behavior of the matrix surface compared with the matrix bulk. And finally, one also cannot discount the effects of particle size and pore size distributions (Nimmo, 2013), further complicating the fluid transport through complex porous matrixes.

These results provide important insights in developing time-sensitive responses to oil spills, where both surface and bulk influences may need to be considered when developing suitable materials to hinder progress of the spill.

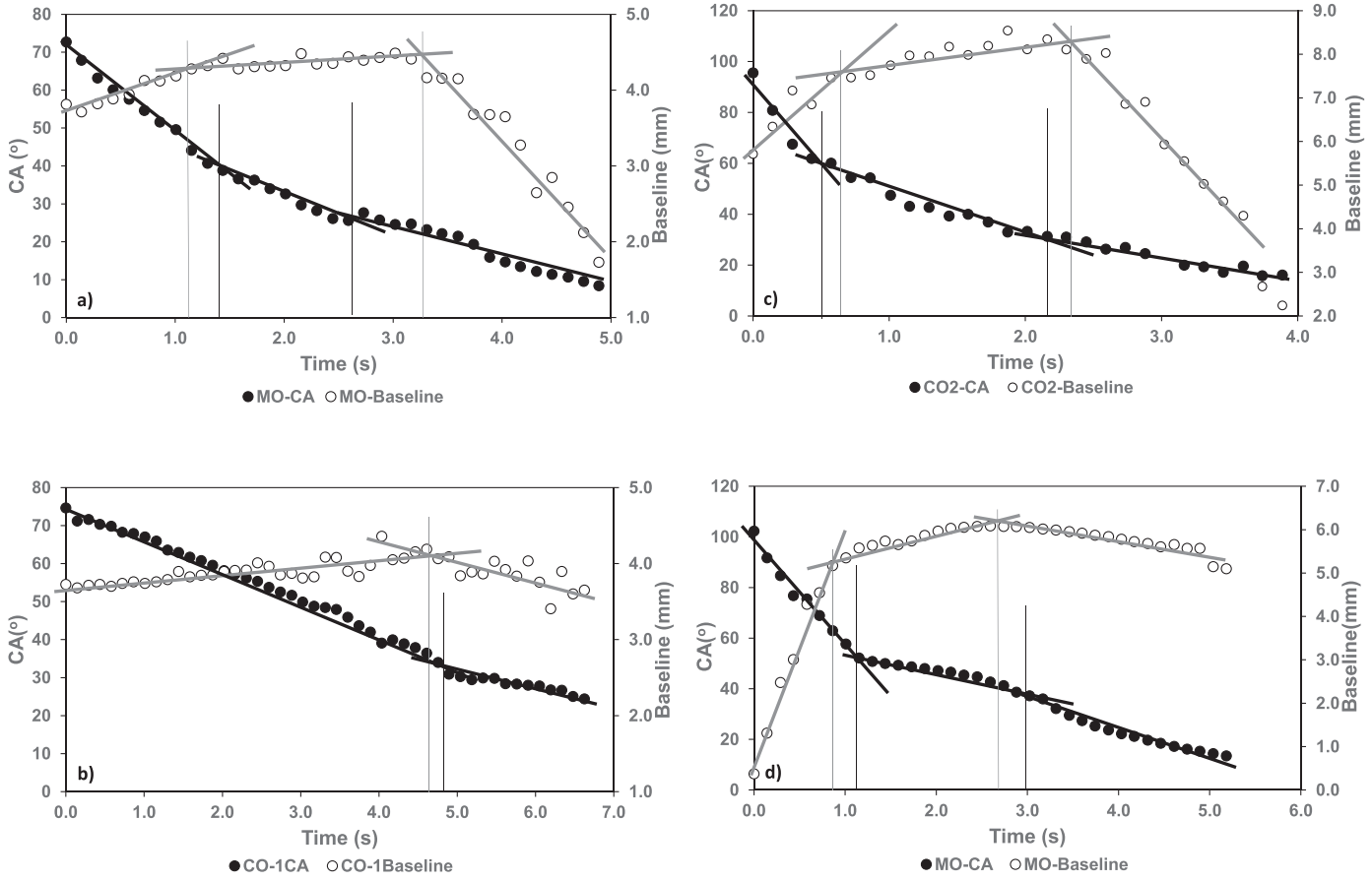

Fig. 5. CA and baseline profiles for various conditions of oil droplets spreading over porous matrixes. a) MO oil on topsoil matrix, 5% MC; b) CO-1 oil on clay matrix, 0% MC; c) CO-2 oil on sand matrix, 5% MC; d) MO oil on mixture matrix, 10% MC.

3.4. Comparison of findings with flow models of liquid droplets over porous materials

CA and baseline data vs time are measurements commonly utilized to develop empirical or numerical models of fluid flow behavior over porous substrates. Several studies (Alleborn and Raszillier, 2004; Denesuk et al., 1993; Frank and Perré, 2012; Johnson et al., 2019; Markicevic et al., 2010; Starov, 2004; Starov et al., 2003) describe such systems based on the behavior profiles of these measured variables, and the ability to identify either two or three stages to denote complete or incomplete wetting, respectively. Here, we focus on exploring the profiles obtained to help explain the fluid flow behavior observed in our experimental investigation. Fig. 5 shows examples of overlaid baseline and CA data with time for four of 36 different conditions investigated. These examples cover the array of variables tested (matrix components, MC, oil viscosity) and demonstrate the complete and incomplete wetting profiles as described by others (Arjmandi-Tash et al., 2017; Johnson et al., 2019; Starov, 2004; Starov et al., 2003).

In all 36 conditions considered, only five were 'not classifiable', meaning that there were different numbers of sections between the CA and baseline profiles, or the change to a new section did not correspond with both profiles. Sections within CA and baseline profiles 'corresponded' if they both began or ended within 1s of each other. Of the remaining 31 conditions, 16% demonstrated complete wetting profiles while 84% conformed to incomplete wetting profiles. Of the complete wetting cases, all but one case was observed at 0% MC. Of the five 'not classifiable' cases, three of these occurred with mixture matrixes, substrates that were the most chemically complex and heterogeneous as they contained multiple components.

While the majority of cases such as those shown in Fig. 5 were identified as complete (two sections) or incomplete (three sections) wetting, their profile shapes frequently did not follow those described by Johnson et al. (2019) and Starov et al. (2003). For example, with the incomplete wetting cases, the middle stage should conform to an approximately constant baseline value, and the third stage should demonstrate an approximately constant CA value. The first stage should also be quite rapid. This behavior was evident in some, but certainly not all, cases investigated, and it is possible that chemically complex and thick porous matrixes may not in fact conform as closely to the models proposed. In those studies cited (Johnson et al., 2019; Starov et al., 2003), the thick porous substrates were glass or metal filters, and sponges, all of which were prepared from chemically homogeneous materials. In the current study, each matrix was chemically heterogeneous even with the individual component matrixes (though dominant in the named component), let alone when combined as the mixture matrix. Additionally, these substrates were physically present in compact particulate form, whereas the filters and sponge were a single, continuous material.

Raw data was converted to dimensionless parameters and further explored to test the claims of universality of baseline and CA with time (Johnson et al., 2019; Starov, 2004; Starov et al., 2003). Time was divided by the maximum spreading time; baseline by the maximum baseline recorded; and CA by that recorded at the maximum baseline, in keeping with that described by Starov et al. (2003). Sand was likely to be the most chemically homogeneous of the component matrixes, since topsoil and clay were still mixtures of soil, though dominant in their respective components of silt and clay. Consequently, the dimensionless CA and baseline curves for sand were the most likely to follow universal behavior, as shown in Fig. 6, for 0, 5 and 10% MC. The CA universality

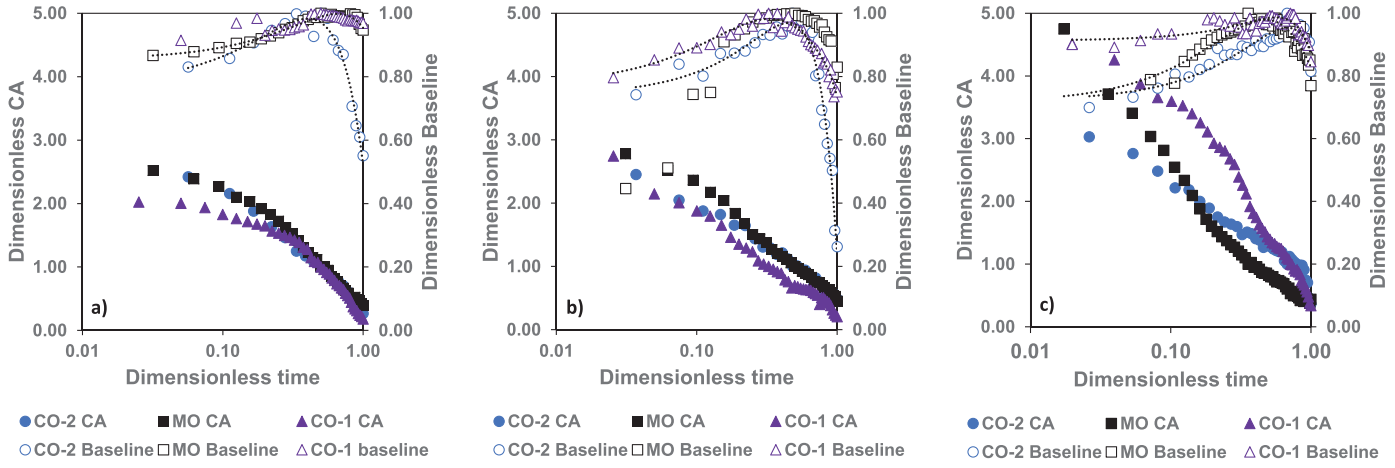

Fig. 6. Dimensionless profiles of CA and baseline data for sand matrixes at a) 0% MC; b) 5% MC and c) 10% MC, for each of the three oils under investigation. Baseline was made dimensionless by dividing the values by the maximum baseline for each trial; CA was made dimensionless by dividing the values by the CA recorded at the maximum baseline. Dotted lines represent lines of best fit through some of the baseline curves.

became increasingly worse as more water was added, due to increasing heterogeneity of the matrix and changes to porosity (Abed Gatea Al-Shammary et al., 2020). Additionally, the baseline universality was observed more closely for low and high viscosity oils (CO-2 and CO-1) compared with medium viscosity oil (MO). As explained earlier, the various additives introduced in MO were found to account for different flow behavior for this oil. Data for the clay matrix at 0% MC and the mixture matrix at 5% MC also somewhat demonstrated universality of data, but all other conditions showed obvious deviations from this behavior.

It is worth noting that much of the experimental data presented by Starov et al. (2003) demonstrated complete wetting of silicone oils over thick substrates, and the only incomplete wetting cases were again on thin porous substrates. In a study by Johnson et al. (2019), additional work was presented for surfactant solutions over thick porous substrates – sponges. While this work followed universal behavior, the behavior profiles again conformed to complete wetting, potentially due to the surface-tension altering properties of the surfactant in the solutions investigated. Alleborn and Raszillier (2004) presented a numerical model of liquid droplets spreading over thick, porous substrates. Their model was governed by Navier-Stokes Eq.s for incompressible Newtonian fluids, as well as Darcy's law to describe the imbibition process. There were several key differences in this model compared with that presented by Starov et al. (2003). One key difference was that using the lubrication theory approximation, fluid motion was restricted to the vertical dimension only, however the position of the wetting front with time was represented laterally. During the sorption of the droplet into the porous substrate, the wetting front advancement was delayed, but increased later on to reach a local maximum before decreasing rapidly when the droplet was completely absorbed (Alleborn and Raszillier, 2004). In the work by Starov et al. (2003), there was a rapid increase in baseline (and corresponding rapid decrease in CA) in the first stage of wetting governed by hydrodynamics, prior to the imbibition process taking place for incomplete wetting cases. Much of Starov et al. (2003) theory was governed by the complete wetting process, developed on two baseline velocity equations representing the increase, and then decrease, of this front. Consequently, the latter described theory tended to predict a maximum baseline much sooner into the wetting process than the former, due to the incorporation of lateral spreading, prior to imbibition, taking place. This may well be applicable for thin porous substrates where lateral spreading is more expected, but for thick porous substrates, one would expect the imbibition or sorption process to be more dominant.

The descriptive results from the numerical simulations by Alleborn and Raszillier (2004) tended to match the profiles observed in Fig. 6, where a relatively constant baseline is predicted at early times, followed by a later maximum. More than 70% of cases investigated in the current study confirmed that the maximum baseline was not reached until at least half-way into the total penetration time of the droplet, with 30% of cases not reaching the maximum until 75% of the penetration time. Additionally, the lateral spreading as confirmed by differences between maximum and initial baseline showed that there was much less lateral movement of oils as the viscosity increased.

Experimental findings from the present work tended to reveal a difference in oil spreading and penetration behavior at the surface compared with the bulk, and was linked to properties such as porosity that differ substantially at these two positions. A numerical development discussed by Markicevic et al. (2010) identified a primary spreading of a sessile drop comprising of two parts: the droplet on the surface of the medium and the liquid imbibing into the porous medium; and a secondary spreading of the liquid when there was no longer a sessile droplet remaining on the surface. All three situations were modeled using a dynamic capillary network model, and backed by experiment using sand medium and a nerve chemical warfare agent, with similar viscosity and surface tension to CO-2. Using the case of a constant droplet baseline being depleted into the porous material, Markicevic et al. (2010) confirmed experimental data with the model by the introduction of a remnant liquid layer remaining on the surface. This was first suggested by Denesuk et al. (1993), where a very thin film remained while the CA of the droplet reduced. It is plausible that this remnant film, if present, may also contribute to observed differences in spreading behavior of liquids on the surface compared with through the bulk.

Finally, the times taken to reach a maximum baseline and a CA of 20° in the present study *were* influenced by the matrix type, oil type, and MC. The various models reviewed here that directly rely on baseline and CA data did not consider these influences except the work of Starov and others (Johnson et al., 2019; Starov, 2004; Starov et al., 2003), where universality of conditions was concluded. The variables investigated (matrix type, oil type, and MC) were found to be statistically significant in many cases regarding their influence on CA and baseline observations, and therefore future modeling work of fluid flow over porous media should consider incorporating these additional influences.

4. Conclusions

This study sought to investigate fluid flow behavior of oils often found in oil spills, over realistic soil-based matrixes, to better understand both surface and bulk variables that influence spreading phenomena on realistic, porous, chemically heterogeneous, thick, and rough surfaces.

Results from spreading kinetics studies of oils flowing through soil substrates revealed quicker spreading times and larger areas of oil spread through the matrix depth for low viscosity oils, dry, and loosely packed matrixes. All three variables were deemed statistically significant in influencing the time of first recorded spread, while only the MC was significant for the spreading area, suggesting oil-water immiscibility phenomena at play.

Results from surface interaction studies between the substrate and oil demonstrated that the initial CA was strongly influenced by MC and matrix components, while initial and maximum baselines were influenced only by the oil type. This suggests lateral spread was dependent on the oil viscosity, while initial CA was more dependent on the substrate conditions. Clay matrixes tended to reduce the initial CA measured, while increased MC caused the initial CA to increase. Larger initial and maximum baselines tended to be recorded for the lower viscosity oils, along with wider lateral spreading, compared with the medium and high viscosity oils. Penetration of the oil droplets, quantified by the time taken to reach a CA of 20^{o} and maximum baseline, was influenced by the matrix type, oil type, and MC, in that order. Surprisingly, penetration times were quicker at higher MC, in contradiction to the spreading kinetics studies, leading to the conclusion of different spreading behavior at the surface compared with the bulk.

Surface measurements best matched literature models that described fluid flow over thick porous substrates, where vertical spreading from capillary forces was initially more dominant than lateral spreading. Universality of fluid flow behavior, regardless of oil viscosity, substrate material, or thickness, was generally not supported with the present results. Thick, complex matrixes with considerable chemical heterogeneity, MC, porosity, and surface roughness, as well as liquids that were chemically complex, showed statistically significant influences on CA and baseline data. Hence it is recommended that future numerical models incorporate these additional effects when describing fluid flow behavior over porous substrates.

Furthermore, this study shed new light on understanding and identifying several surface factors that influence the spread of oils over soil-based matrixes that were previously thought not to influence fluid flow behavior. These important findings will help shape the development of future materials or spill containment methods to minimize spread and long-term damage to the soil habitat.

Authors' contributions

Mr. Firoz Ahmed performed all the experimental work and generated graphs of the raw data, and was responsible for writing early drafts of the introduction and methodology sections of the paper. Dr. Brenda Hutton-Prager was responsible for the conceptual development of this work, and performed the statistical analyses which led to identification of several variables responsible for bulk and surface fluid flow. She also discussed the present experimental findings with various theoretical models proposed in the literature, further enabling additional insights into the many influences that govern oil spreading over soils. Both authors worked together to produce the final manuscript.

Declaration of Competing Interest

The authors declare that they have no known competing financial interests or personal relationships that could have appeared to influence the work reported in this paper.

Acknowledgements

Internal funding from the University of Mississippi helped support this work. This research did not receive any specific grant from funding agencies in the public, commercial, or not-for-profit sectors.

The authors wish to thank undergraduate students Jasmine Stevens and Justin Puhnaty for their assistance with some of the experimental work.

References

Abed Gatea Al-Shammary, A., Kouzani, A., Gyasi-Agyei, Y., Gates, W., Rodrigo-Comino, J., 2020. Effects of solarisation on soil thermal-physical properties under different soil treatments: a review. Geoderma 363, 114137. doi:10.1016/j.geoderma.2019.114137.

Alleborn, N., Raszillier, H., 2004. Spreading and sorption of a droplet on a porous substrate. Chem. Eng. Sci. 59, 2071–2088. doi:10.1016/j.ces.2004.02.006.

Arjmandi-Tash, O., Kovalchuk, N.M., Trybala, A., Kuchin, I.V., Starov, V., 2017. Kinetics of wetting and spreading of droplets over various substrates. Langmuir 33, 4367–4385. doi:10.1021/acs.langmuir.6b04094.

Bowling, S.R., Khasawneh, M.T., Kaewkuekool, S., Cho, B.R., 2009. A logistic approximation to the cumulative normal distribution. J. Ind. Eng. Manag. 2, 114–127. doi:10.3926/jiem.2009.v2n1.p114-127.

Chen, J., Zhang, W., Wan, Z., Li, S., Huang, T., Fei, Y., 2019. Oil spills from global tankers: status review and future governance. J. Clean. Prod. 227, 20–32. doi:10.1016/j.jclepro.2019.04.020.

Chinenyeze, M.A.J., Ekene, U.R., 2015. Physical and chemical properties of crude oils and their geologic significances. Int. J. Sci. Res. 6, 8.

Cummins, B.M., Chinthapatla, R., Ligler, F.S., Walker, G.M., 2017. Time-dependent model for fluid flow in porous materials with multiple pore sizes. Anal. Chem. 89, 4377–4381. doi:10.1021/acs.analchem.6b04717.

Curry, C.W., Bennett, R.H., Hulbert, M.H., Curry, K.J., Faas, R.W., 2004. Comparative study of sand porosity and a technique for determining porosity of undisturbed marine sediment. Mar. Georesources Geotechnol. 22, 231–252. doi:10.1080/10641190490900844.

Das, S., Patel, H.V., Milacic, E., Deen, N.G., Kuipers, J.A.M., 2018. Droplet spreading and capillary imbibition in a porous medium: a coupled IB-VOF method based numerical study. Phys. Fluids 30, 012112. doi:10.1063/1.5010716.

Denesuk, M., Smith, G.L., Zelinski, B.J.J., Kreidl, N.J., Uhlmann, D.R., 1993. Capillary penetration of liquid droplets into porous materials. J. Colloid Interface Sci. 158, 114–120. doi:10.1006/jcis.1993.1235.

Djomgoue, P., Njopwouo, D., 2013. FT-IR Spectroscopy Applied For Surface Clays Characterization. J. Surf. Eng. Mater. Adv. Technol. 03, 275–282. doi:10.4236/jsemat.2013.34037.

Frank, X., Perré, P., 2012. Droplet spreading on a porous surface: a lattice Boltzmann study. Phys. Fluids 24, 042101. doi:10.1063/1.3701996.

Ghanbarian, B., Hunt, A., Daigle, H., 2016. Fluid flow in porous media with rough pore-solid interface. Water Resour. Res. 52, 2045–2058. doi:10.1002/2015WR017857.

Guimarães, B.C.M., Arends, J.B.A., van der Ha, D., Van de Wiele, T., Boon, N., Verstraete, W., 2010. Microbial services and their management: recent progresses in soil bioremediation technology. Appl. Soil Ecol. 46, 157–167. doi:10.1016/j.apsoil.2010.06.018.

Hamad, A., Al-Zubaidy, E., Fayed, M.E., 2004. Assessment of used motor oil recycling opportunities in the United Arab Emirates. J. King Saud Univ. - Eng. Sci. 16, 215–227. doi:10.1016/S1018-3639(18)30788-8.

Herdan, J.M., 1997. Lubricating oil additives and the environment — an overview. Lubr. Sci. 9, 161–172. doi:10.1002/ls.3010090205.

Jernelöv, A., 2010. The Threats from oil spills: now, then, and in the future. AMBIO 39, 353–366. doi:10.1007/s13280-010-0085-5.

Johnson, P., Trybala, A., Starov, V., 2019. Kinetics of spreading over porous substrates. Colloids Interf. 3, 38. doi:10.3390/colloids3010038.

Katusich, O., Vallone, A., Blasetti, H., Alassia, F., Ríos, S.M., Sapag, K., Nudelman, N., 2016. Evaluation of sorptive capacity of natural clay, pillared clay, and alga-modified clay to contain oil spills in soil. Int. J. Mod. Chem. Eng. 2, 15–25.

Kettler, T.A., Doran, J.W., Gilbert, T.L., 2001. Simplified method for soil particle-size determination to accompany soil-quality analyses. Soil Sci. Soc. Am. J. 65, 849–852. doi:10.2136/sssaj2001.653849x.

Kiefer, J., Rasul, N., Ghosh, P., von Lieres, E., 2013. Surface and bulk porosity mapping of polymer membranes using infrared spectroscopy. J. Membr. Sci. 452, 152–156. doi:10.1016/j.memsci.2013.10.022.

Klamerus-Iwan, A., Błońska, E., Lasota, J., Kalandyk, A., Waligórski, P., 2015. Influence of oil contamination on physical and biological properties of forest soil after chainsaw use. Water. Air. Soil Pollut. 226, 389. doi:10.1007/s11270-015-2649-2.

Knox, R.C., Sabatini, D.A., Harwell, J.H., Brown, R.E., West, C.C., Blaha, F., Griffin, C., 1997. Surfactant remediation field demonstration using a vertical circulation well. Ground Water 35, 948–953. doi:10.1111/j.1745-6584.1997.tb00166.x.

Lee, W., Kang, P., Kim, A., Lee, S., 2018. Impact of surface porosity on water flux and structural parameter in forward osmosis. Desalination 439, 46–57. doi:10.1016/j.desal.2018.03.027.

Lim, M.W., Lau, E.V., Poh, P.E., 2016. A comprehensive guide of remediation technologies for oil contaminated soil — present works and future directions. Mar. Pollut. Bull. 109, 14–45. doi:10.1016/j.marpolbul.2016.04.023.

Markicevic, B., D'Onofrio, T., Navaz, H., 2010. On spread extent of sessile droplet into porous medium: numerical solution and comparisons with experiments. Phys. Fluids 22, 012103. doi:10.1063/1.3284782.

Matko, V., 2003. Odredivanje poroznosti primjenom stohastičke metode. Autom. J. Control Meas. Electron. Comput. Commun. Koremaferhr. 44, 3–4.

Milne, A.J.B., Amirfazli, A., 2012. The Cassie Eq.: How it is meant to be used. Adv. Colloid Interface Sci. 170, 48–55. doi:10.1016/j.cis.2011.12.001.

Mohamed, A.M.A., Abdullah, A.M., Younan, N.A., 2015. Corrosion behavior of superhydrophobic surfaces: a review. Arab. J. Chem. 8, 749–765. doi:10.1016/j.arabjc.2014.03.006.

Nimmo, J.R., 2013. Porosity and pore-size distribution. Earth Systems andEnvi. Sci, 9. Elsevier doi:10.1016/B978-0-12-409548-9.05265-9.

Ramadass, K., Megharaj, M., Venkateswarlu, K., Naidu, R., 2015. Ecological implications of motor oil pollution: earthworm survival and soil health. Soil Biol. Biochem. 85, 72–81. doi:10.1016/j.soilbio.2015.02.026.

Razmjoo, K., Adavi, Z., 2012. Assessment of bermudagrass cultivars for phytoremediation of petroleum contaminated soils. Int. J. Phytoremediation 14, 14–23. doi:10.1080/15226514.2011.560212.

Ritchey, E.L., McGrath, J.M., Gehring, D., 2015. Determining soil texture by feel. Agric. Nat. Resour. Publ. 4, 139. https://uknowledge.uky.edu/anr_reports/139.

Rutter, T., Hutton-Prager, B., 2018. Investigation of hydrophobic coatings on cellulose-fiber substrates with in-situ polymerization of silane/siloxane mixtures. Int. J. Adhes. Adhes. 86, 13–21. doi:10.1016/j.ijadhadh.2018.07.008.

Savage, D., Liu, J., 2015. Water/clay ratio, clay porosity models and impacts upon clay transformations. Appl. Clay Sci. 116–117, 16–22. doi:10.1016/j.clay.2015.08.011.

Schraer, S.M., Shaw, D.R., Boyette, M., Kingery, W.L., Koger, C.H., 2003. Sorption–desorption of cyanazine in three mississippi delta soils. Weed Sci 51, 635–639 10.1614/0043-1745(2003)051[0635:SOCITM]2.0.CO;2.

Song, K., Lee, J., Choi, S.-O., Kim, J., 2019. Interaction of surface energy components between solid and liquid on wettability, and its application to textile anti-wetting finish. Polymers 11, 498. doi:10.3390/polym11030498.

Starov, V.M., 2004. Surfactant solutions and porous substrates: spreading and imbibition. Adv. Colloid Interface Sci. 111, 3–27. doi:10.1016/j.cis.2004.07.007.

Starov, V.M., Zhdanov, S.A., Kosvintsev, S.R., Sobolev, V.D., Velarde, M.G., 2003. Spreading of liquid drops over porous substrates. Adv. Colloid Interface Sci. 104, 123–158. doi:10.1016/S0001-8686(03)00039-3.

Stone, R., 1995. Russian arctic battles pipeline leak. Science 268, 796–797. doi:10.1126/science.268.5212.796.

Uddin, F., 2008. Clays, nanoclays, and montmorillonite minerals. Metall. Mater. Trans. A 39, 2804–2814. doi:10.1007/s11661-008-9603-5.

USDOE Energy Information Administration, 1995. Oil and gas resources of the Fergana Basin (Uzbekistan, Tadzhikistan, and Kyrgyzstan) (No. DOE/EIA-TR/0575).Office of Oil and Gas. https://doi.org/10.2172/10103777

Wang, Y., Feng, J., Lin, Q., Lyu, X., Wang, X., Wang, G., 2013. Effects of crude oil contamination on soil physical and chemical properties in Momoge wetland of China. Chin. Geogr. Sci. 23, 708–715. doi:10.1007/s11769-013-0641-6.